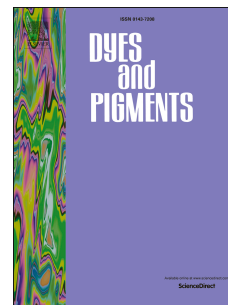


Accepted Manuscript

Deep red emitting triphenylamine based coumarin-rhodamine hybrids with large Stokes shift and viscosity sensing: Synthesis, photophysical properties and DFT studies of their spirocyclic and open forms

Shantaram Kothavale, Amol G. Jadhav, Nagaiyan Sekar



PII: S0143-7208(16)30792-6

DOI: [10.1016/j.dyepig.2016.11.010](https://doi.org/10.1016/j.dyepig.2016.11.010)

Reference: DYPI 5579

To appear in: *Dyes and Pigments*

Received Date: 21 September 2016

Revised Date: 8 November 2016

Accepted Date: 8 November 2016

Please cite this article as: Kothavale S, Jadhav AG, Sekar N, Deep red emitting triphenylamine based coumarin-rhodamine hybrids with large Stokes shift and viscosity sensing: Synthesis, photophysical properties and DFT studies of their spirocyclic and open forms, *Dyes and Pigments* (2016), doi: 10.1016/j.dyepig.2016.11.010.

This is a PDF file of an unedited manuscript that has been accepted for publication. As a service to our customers we are providing this early version of the manuscript. The manuscript will undergo copyediting, typesetting, and review of the resulting proof before it is published in its final form. Please note that during the production process errors may be discovered which could affect the content, and all legal disclaimers that apply to the journal pertain.

Deep red emitting triphenylamine based coumarin-rhodamine hybrids with large Stokes shift and viscosity sensing: Synthesis, photophysical properties and DFT studies of their spirocyclic and open forms

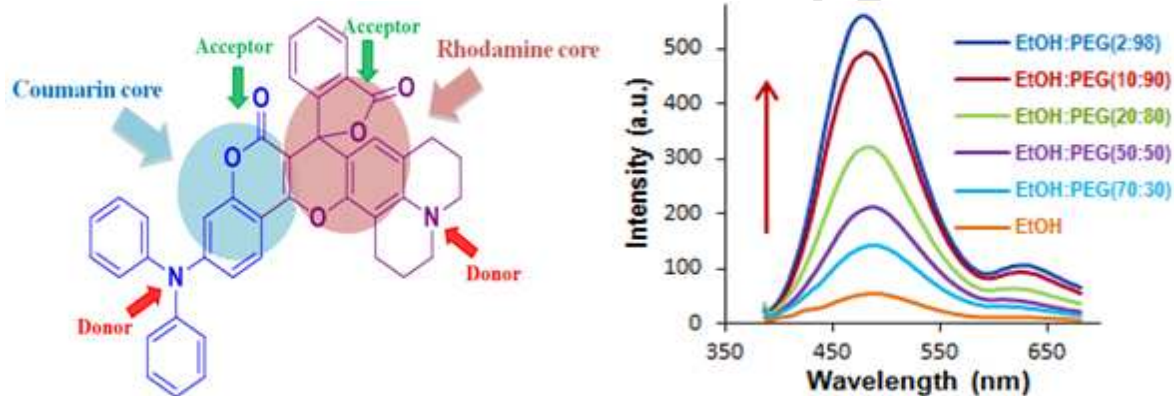
Shantaram Kothavale, Amol G. Jadhav, Nagaiyan Sekar*

Department of Dyestuff Technology, Institute of Chemical Technology, Matunga,
Mumbai-400 019, India.

E-mail: n.sekar@ictmumbai.edu.in, nethi.sekar@gmail.com

Tel: +91 22 3361 2707; Fax: +91 22 3361 1020.

Graphical Abstract



Deep red emitting triphenylamine based coumarin-rhodamine hybrids with large Stokes shift and viscosity sensing: Synthesis, photophysical properties and DFT studies of their spirocyclic and open forms

Shantaram Kothavale, Amol G. Jadhav, Nagaiyan Sekar*

Department of Dyestuff Technology, Institute of Chemical Technology, Matunga,
Mumbai-400 019, India.

E-mail: n.sekar@ictmumbai.edu.in, nethi.sekar@gmail.com

Tel: +91 22 3361 2707; Fax: +91 22 3361 1020.

Abstract

We designed and synthesized triphenylamine based and coumarin fused rhodamine hybrid dyes and characterized using ^1H , ^{13}C NMR and HR-LCMS analysis. Both the newly synthesized hybrid dyes were found to show red shifted absorption as well as emissions and large Stokes shift (40-68 nm) as compared to the small Stokes shift (25-30 nm) of reported dyes Rhodamine **B** and **101**. Photophysical properties of these dyes were studied in different solvents and according to the solvents acidity or basicity they preferred to remain in their spirocyclic or open form in different ratio. We studied the spirocyclic as well as open form derivatives of these dyes for their viscosity sensitivity in three different mixture of solvents i.e. polar-protic [EtOH-PEG 400], polar-aprotic [toluene-PEG 400] and non-polar-aprotic [toluene-paraffin]. They are found to show very high viscosity sensitivity in polar-protic mixture of solvents [EtOH-PEG 400] and hence concluded that both polarity as well as viscosity factor worked together for the higher emission enhancement rather than only viscosity factor. As these dyes showed very high viscosity sensitivity in their spirocyclic as well as open form, they can be utilized as viscosity

sensors in visible as well as deep red region. We also correlated our experimental finding theoretically by using Density Functional theory computations.

Keywords: Coumarin rhodamine hybrids, solvatochromism, viscosity sensitivity, deep red emitting dyes, Density functional theory (DFT).

Introduction

Fluorescent environment sensitive dyes such as molecular rotors are widely used to measure viscosity in biological systems in place of conventional methods due to its advantages such as small sample volume and high speed of the readout [1–3]. Hence currently fluorescent molecular probes are the most suitable tools for real-time measurements of viscosity in both micro- and macro systems [4,5]. Molecular rotors are a group of fluorescent compounds that consists of an electron donor group in π -conjugation with an electron acceptor group which form twisted intramolecular charge transfer (TICT) states after excitation. In such cases fluorescence quenching via an internal non-radiative process that involves molecular rotation between the donor and the acceptor (TICT) is observed which is hindered in highly viscous environment to regain the fluorescence emission [6,7]. 9-Dicyanovinyl)-julolidine (DCVJ) and its different derivatives have been extensively studied for their viscosity sensitivity which are weakly fluorescent initially due to the fast rotation around the single bond interconnecting the julolidine and dicyanovinyl subunits [8–13]. Freely rotating phenyl ring at meso position in BODIPY dye is also utilized for application as viscosity sensors [14–17].

Though some highly fluorescent dyes like rhodamine, fluorescein, BODIPY and cyanine derivatives have been widely used as fluorescent probes[18,19], labels[20–22], logic gates

[23,24], light-emitting materials [25–28], and light-harvesting systems [29–32], they have the serious disadvantage of very small Stokes shifts (typically less than 25 nm), which can lead to serious self-quenching and fluorescence detection errors because of excitation backscattering effects [33,34]. The large Stokes shift could reduce self-absorption as well as obtain high resolution and low detection limits. Therefore, it remains highly desirable to explore new design strategies for the development of deep red fluorescent dyes with great photo stability and large Stokes shift while being used as ratiometric sensing platforms.

Similarly deep red emitting or NIR fluorescent probes are attractive for biological applications because of minimum photo damage to biological samples, deep tissue penetration, and minimum interference from the background auto fluorescence of biomolecules in the living systems [35,36]. Rhodamine dyes due to their excellent photophysical properties, such as high molar extinction coefficients, excellent fluorescence quantum yields, and great photo stability, are widely used as fluorescent probes and molecular markers in chemistry and biology [37–39]. However, the absorption and emission wavelengths of most rhodamine derivatives are below 600 nm and exhibit a very small Stokes shift (rhodamine B: 19 nm) which is sometimes unsuitable for biological applications due to self-absorption. Many efforts have been made to acquire longer-wavelength rhodamine derivatives, including extending the conjugation of the xanthene ring, replacing the central carbon with a nitrogen atom or introducing a cyano group on the central carbon atom, as well as replacing the oxygen bridge atom by other elements, such as N, C, S, and Se [40,41]. However, rhodamine analogues developed by these strategies are very difficult to synthesize.

Hence currently trend to hybridize two totally different dyes with unique photophysical properties is being rapidly accepted by researchers to obtain the hybrid dye with desired

photophysical properties. For example, ESIPT-BODIPY [42,43], ESIPT-Coumarin [44,45], BODIPY-Coumarin [46,47], BODIPY-Rhodamine [48,49] and Coumarin- Rhodamine [50] dyes were synthesized successfully and found to show better photophysical properties than their precursors. Recently P. Wang and coworkers synthesized fused coumarin-rhodamine hybrid dyes and utilized them for bioimaging study in the NIR region. The new hybrid dyes not only retained the advantages of coumarin and rhodamine individual derivatives in themselves but also found to show larger Stokes shift and red shifted emission wavelengths [50].

In this work, we have successfully synthesized triphenylamine based two novel deep red emitting coumarin-rhodamine hybrid fluorescent dyes. Environment friendly deep eutectic ionic liquid i.e. NMP.HSO₄ is used as the reaction media to obtain the coumarin fused rhodamine dyes in good yield instead of using traditional highly concentrated acids. As TICT is responsible for the viscosity sensitivity we designed the dyes so that triphenylamine can be used as main donor from coumarin side and *N,N* diethyl aniline or julolidine as main donors from rhodamine side. The pure dyes in their spirocyclic form were studied for their viscosity sensitivity in polar protic [EtOH-PEG 400], aprotic polar [toluene-PEG 400] and aprotic non-polar [toluene-paraffin] viscous media in the presence and absence of TFA. A substantial change in the emission intensities in the visible as well as deep red region were observed for both the dyes particularly in the polar viscous medium [EtOH-PEG 400]. **Fig. 1** represents the structure of hybrid dyes **Cou-Rh-1** and **Cou-Rh-2** in their spirocyclic as well as open form.

<< Please insert **Fig. 1**. Structure of the coumarin-rhodamine hybrid dyes **Cou-Rh-1** and **Cou-Rh-2** >>

2. Experimental section

2.1 Materials and equipments

All the reagents and solvents were purchased from S d Fine Chemical Limited, Mumbai, India and used without further purification. The reactions were monitored by TLC using on 0.25 mm E-Merck silica gel 60 F254 precoated plates, which were visualized with UV light. ^1H and ^{13}C NMR spectra were recorded on a Varian Cary Eclipse Australia using TMS (Tetramethylsilane) as an internal standard. High resolution liquid chromatography mass spectra were recorded on 6550 iFunnel QTOF LC/MS spectrometer from Agilent Technologies. The absorption spectra of the compounds were recorded on a PerkinElmer UV- visible spectrophotometer Lambda 25. Fluorescence emission spectra were recorded on Varian Cary Eclipse fluorescence spectrophotometer using freshly prepared solutions at the concentration of $1 \times 10^{-6} \text{ mol L}^{-1}$. Melting points were measured on standard melting point apparatus from Sunder Industrial Product Mumbai and are uncorrected.

2.2 Computational Methods

Density Functional Theory (DFT) [51] was utilized to optimize ground state (S_0) geometries of all the compounds using the Gaussian 09 package and the popular hybrid functional B3LYP. The B3LYP combines Becke's three parameter exchange functional (B3)[52] with the nonlocal correlation functional by Lee, Yang, and Parr (LYP) [53]. In both the methods DFT and time-dependent density functional theory (TD-DFT), same basis set i.e. 6-31G (d) was used. The low-lying first singlet excited states (S_1) of the dyes were relaxed to obtain their minimum energy geometries using the TD-DFT in their gas phase. By using TD-DFT at the same hybrid functional and basis set, the vertical excitation energies and oscillator strengths were obtained for the lowest 10 singlet-singlet transitions at the optimized ground state equilibrium geometries

[54]. Optimized ground state structures were utilized to obtain the electronic absorption spectra, including maximum absorption and oscillator strengths.

<< Please insert **Scheme 1**: Synthesis of coumarin-rhodamine hybrids **Cou-Rh-1** and **Cou-Rh-2**

>>

2.3 Synthetic strategy

We synthesized methoxy triphenylamine intermediate 2 starting from aniline utilizing Buchwald reaction condition, which was further de-methylated to acquire intermediate 3 by using pyridine.HCl as de-methylating reagent. At the same time intermediate 10 was synthesized starting from 2, 4, 6 tri-chlorophenol (9) using reported procedure [55]. Intermediate 3 was reacted with intermediate 10 to get triphenylamine based 4-hydroxyl coumarin derivative (4). We also synthesized keto-acid intermediates 6 and 8 following the reported procedures [56,57] and treated with coumarin intermediate 4 in ionic liquid HNMP.HSO₄ as reaction media to get the desired coumarin-rhodamine hybrids **Cou-Rh-1** and **Cou-Rh-2** in their spirocyclic form. HNMP.HSO₄ act as reaction medium as well as acid catalyst for the synthesis of desired coumarin fused rhodamine derivatives. We further converted the spirocyclic form of **Cou-Rh-1** and **Cou-Rh-2** dyes into their respective open form by treating them with MeOH.HCl solution, in which they get immediately converted into their respective open form hydrochloride salt form. This procedure was repeated twice and the solvent was evaporated on rotavapour to get shiny reddish black colored open salt form derivatives of **Cou-Rh-1** and **Cou-Rh-2**.

2.4 Synthesis and Characterization

2.4.1 Synthesis of 3-methoxy-N,N-diphenylaniline (2)

Same procedure as reported from our group[58] was followed.

2.4.2 Synthesis of 3-(diphenylamino)phenol (**3**)

3-Methoxy-*N,N*-diphenylaniline **2** (16 g, 58.2 mmol) was dissolved in 80 g of pyridine. HCl and heated to 200 °C for 10 hrs. After cooling to room temperature, water was added in the reaction mass and solid precipitated out was filtered, dried well and collected as crude product, which was further purified on column chromatography using 10% ethyl acetate in hexane as the eluent to get the pure product.

Yield: 12 g, (79 %); Melting point = 98 – 100 °C

¹H NMR (500 MHz, CDCl₃) δ 4.60 (s, 1H), 6.46 (dd, *J* = 8 and 2 Hz, 1H), 6.52 (t, *J* = 2 Hz, 1H), 6.65 (dd, *J* = 8 and 2 Hz, 1H), 7.01-7.07 (m, 2H), 7.09-7.11 (m, 4H), 7.23-7.27 (m, 4H), ¹³C NMR (126 MHz, CDCl₃) δ 109.4, 110.4, 116.1, 123.1, 124.7, 129.3, 130.1, 147.6, 149.3, 156.2. Elemental analysis calcd (%); Mol. formula: C₁₈H₁₅NO (C: 82.73, H: 5.79, N: 5.36, O: 6.12; found: C: 82.68, H: 5.81, N: 5.32, O: 6.08).

2.4.3 Synthesis of 7-(diphenylamino)-4-hydroxy-2H-chromen-2-one (**4**)

3-(Diphenylamino) phenol **3** (5 g, 19.1 mmol) and diphenylmalonate **8** (9.7 g, 21 mmol) were added into anhydrous toluene (20 mL). The mixture was heated to reflux for overnight, and after completion the reaction mass was cooled to room temperature. The solid precipitated out was filtered as pure product.

Yield: 3.6 g (57 %) Melting point = 258 – 262 °C

¹H NMR (500 MHz, DMSO-*d*₆) δ 5.39 (s, 1H), 6.51-6.52 (d, *J* = 2.0, 1H), 6.72-6.45 (dd, *J* = 8.5, 2.5, 1H), 7.15-7.20 (m, 6H), 7.36-7.39 (m, 4H), 7.59-7.61 (d, *J* = 8.5, 1H), 12.20 (s, 1H). ¹³C NMR (126 MHz, DMSO-*d*₆) δ 88.6, 105.5, 108.9, 115.7, 124.6, 125.6, 126.6, 130.4, 146.1,

151.8, 155.3, 162.5, 166.3, 168.8. Elemental analysis calcd (%); Mol. formula: C₂₁H₁₅NO₃ (C: 76.58, H: 4.59, N: 4.25, O: 14.57; found: C: 76.53, H: 4.62, N: 4.19, O: 14.59).

2.4.4 General procedure for the synthesis of coumarin-rhodamine hybrids *Cou-Rh-1* and *Cou-Rh-2*

4-Hydroxy coumarin intermediate 4 was reacted with keto-acid intermediate 6 and 8 in H-NMP.HSO₄ (10 mL) at 90 °C for 14 - 16 hours. After completion the reaction mixture was cooled to room temperature and was poured into 100 mL ice-cold water and stirred for 15 min. The product was extracted with chloroform (100 mL x 3); the organic layer was separated, dried over anhydrous Na₂SO₄ and evaporated over rotary evaporator. The crude product was purified by silica gel (100-200 mesh size) column chromatography using 1-5 % methanol in chloroform to give the respective dyes **Cou-Rh-1** and **Cou-Rh-2**.

Dye Cou-Rh-1:

Yield = 28 %, Melting point: 258 °C

¹H NMR (500 MHz, CDCl₃) δ 1.17 (t, *J* = 7.5 Hz, 6H), 3.34 (q, *J* = 7 Hz, 4H), 6.42 (dd, *J* = 9 and 2.5 Hz, 1H), 6.49 (d, *J* = 2.5 Hz, 1H), 6.57 (d, *J* = 9 Hz, 1H), 6.76 (d, *J* = 2 Hz, 1H), 6.95 (dd, *J* = 9 and 2.5 Hz, 1H), 7.12 (t, *J* = 7.5 Hz, 1H), 7.16-7.19 (m, 5H), 7.33-7.36 (m, 4H), 7.50-7.5 (m, 2H), 7.89 (d, *J* = 8.5 Hz, 1H), 7.98 (d, *J* = 8 Hz, 1H). ¹³C NMR (126 MHz, CDCl₃) δ 12.5, 44.4, 80.2, 96.6, 97.4, 106.2, 110.2, 116.1, 122.3, 124.0, 124.7, 125.3, 126.2, 128.0, 128.9, 129.0, 129.7, 134.0, 145.8, 149.3, 150.5, 152.5, 152.9, 154.7, 158.2, 159.3, 170.0. HRMS (ESI): *m/z* calculated for (M + H)⁺ C₃₉H₃₀N₂O₅ 607.2155; found 607.2176.

Dye Cou-Rh-2:

Yield = 23 %, Melting point: >300 °C. ^1H NMR (500 MHz, CDCl_3) δ 1.75-1.93 (m, 4H), 2.42-2.43 (m, 2H), 2.93 (t, $J = 7$ Hz, 2H), 3.11 (m, 2H), 3.17 (t, $J = 7$ Hz, 2H), 6.01 (s, 1H), 6.51 (d, $J = 2.5$ Hz, 1H), 6.88 (dd, $J = 9$ and 2.5 Hz, 1H), 7.20-7.27 (m, 7H), 7.40-7.43 (m, 4H), 7.55-7.65 (m, 2H), 7.85 (d, $J = 7.5$ Hz, 1H), 7.94 (d, $J = 9$ Hz, 1H). ^{13}C NMR (126 MHz, CDCl_3) δ 25.5, 26.1, 31.8, 35.8, 53.6, 54.2, 85.5, 99.7, 109.3, 110.4, 110.7, 111.9, 120.9, 124.7, 128.0, 129.1, 129.2, 129.8, 130.9, 131.5, 132.3, 134.4, 135.2, 139.8, 149.3, 149.9, 150.4, 157.5, 157.8, 159.2, 162.6, 163.8, 174.5. HRMS (ESI): m/z calculated for $(\text{M} + \text{H})^+$ $\text{C}_{44}\text{H}_{30}\text{N}_2\text{O}_5$ 631.2155; found 631.2174.

3. Result and discussion

3.1 Photophysical properties

We studied the absorption and emission properties of these coumarin-rhodamine hybrid derivatives in their spirocyclic as well as open form in different solvents. The spirocyclic form of these dyes was converted into their open form using MeOH.HCl solution. The solvent was evaporated on rotavapour and the same procedure was repeated twice to get the fully open form derivatives. During photophysical studies after dilution in organic solvents these dyes again preferred to remain in their spirocyclic form, hence we added required amount of TFA till the disappearance of the spirocyclic absorption peak to acquire their complete open form. As there are two main chromophores i.e. coumarin and rhodamine, hence two distinct absorption and emission peaks for both the moieties are expected, but due to their fused hybrid structures they behave as coumarin dye in their spirocyclic form to show absorption peak around 371 nm and emission peak around 430 nm. In their open form they behave as rhodamine dye and show absorption peak at around 610 nm and emission peak at around 670 nm. In DMSO solvent

specifically they preferred to remain in their spirocyclic form even after adding excess TFA. They are colorless solid in their spirocyclic form and are reddish black shiny compounds in their open form. In their spirocyclic as well as open form no much difference in the absorption and emission λ_{\max} is observed between the **Cou-Rh-1** and **Cou-Rh-2** dyes (Fig. 2 and S1). In their open form both **Cou-Rh-1** and **Cou-Rh-2** dyes exhibited comparatively higher Stokes shifts (40-68 nm) as compared to the small Stokes shift of 25-30 nm of reported **RH-B** and **RH-101** dyes (Table 1). Due to their extended length of conjugation and fused structures they also showed highly red shifted absorption and emission peaks than the reported **RH-B** and **RH-101** dyes in their open form (Fig. S2).

<< Please insert Fig. 2: Normalized absorption and emission spectra of dyes **Cou-Rh-1** and **Cou-Rh-2** in their open form >>

As *N,N* diethyl amine donating group in **Cou-Rh-1** dye is replaced by rigid julolidine donor in **Cou-Rh-2** dye, we expect red shift in their absorption and emission λ_{\max} but not much shift in both spirocyclic and open form is observed as like in **RH-B** and **RH-101** reported dyes where when we go from *N,N* diethyl aniline to julolidine donor, red shift of 20 and 22 nm is observed in their absorption as well as emission spectra respectively (Fig. 3). As the role of donating group is not clearly differentiated in the case of these coumarin-rhodamine dyes, the coumarin side triphenylamine donor may have taken part in the spirocyclic ring opening mechanism of rhodamine dye to disturb the main donor-acceptor spirocyclic ring opening mechanism of rhodamine. From the available absorption data of these dyes in their spirocyclic as well as open form we calculated their oscillator strength (f) as well as transition dipole moment (μ_{eg}) by using

reported expressions [59]. In general it is observed that both the dyes showed higher values of oscillator strength and transition dipole moment in their open form as compared to the respective spirocyclic form (Table 1).

<< Please insert Fig. 3: Normalized absorption and emission spectra of **RH-B**, **RH-101**, **Cou-Rh-1** and **Cou-Rh-2** in their open form in chloroform solvent >>

<< Please insert Table 1: photophysical properties of **Cou-Rh-1** and **Cou-Rh-2** in their spirocyclic and open form >>

To check out the effect of solvents in their spirocyclic and open form we studied the photophysical properties of **Cou-Rh-1** and **Cou-Rh-2** dyes in both spirocyclic and open form and it is observed that in both the cases quenching of fluorescence from non-polar to polar solvents is observed (**Fig. 4**). But the red shifted emissions observed in their spirocyclic form suggest that these dyes behave as typical coumarin dyes in their spirocyclic form and as typical rhodamine dyes in their open form. Also it can be predicted that the excited state is highly polar in their spirocyclic form as compared to the ground state and vice versa in the case of their open form derivatives. In their spirocyclic form for both **Cou-Rh-1** and **Cou-Rh-2** dyes in acetone solvent typically red shifted emission λ_{\max} values (497 and 504 nm) and consequently very high Stokes shift of 125 and 133 nm were observed respectively. The molar extinction coefficient values are almost double for both the dyes when we go from spirocyclic to open form suggesting that the energy gain process actually switched on only after the ring opening of the rhodamine dye.

<< Please insert **Fig. 4**: Absorption (a) and emission (b) spectra of **Cou-Rh-1** in different solvents in their spirocyclic form. >>

<< Please insert **Table 2**: Photophysical properties of **Cou-Rh-1** dye in its spirocyclic form in all solvents >>

Dye **Cou-Rh-1** showed higher Stokes shift of 10-15 nm than **Cou-Rh-2** dye in all the tested solvents in their open form, but opposite trend is observed in their spirocyclic form where dye **Cou-Rh-2** showed comparatively higher Stokes shift than dye **Cou-Rh-1** in all solvents (**Table 2-3** and **Table S1-S2**). In their open form, both these dyes **Cou-Rh-1** and **Cou-Rh-2** showed highest Stokes shift of 68 and 54 nm in chloroform solvent respectively. In their spirocyclic form comparatively red shifted emissions were observed for dye **Cou-Rh-2** (435-500 nm) than **Cou-Rh-1** dye (430- 476 nm), while the trend is opposite in their open form where dye **Cou-Rh-1** (641-678 nm) exhibited red shifted emissions than dye **Cou-Rh-2** (639-668 nm). From above observations it is clear that dye **Cou-Rh-2** showed better results in its spirocyclic form while dye **Cou-Rh-1** showed better results in its open form. As very high quenching of fluorescence is observed for dye **Cou-Rh-1** in its spirocyclic form than dye **Cou-Rh-2** (**Fig. 4** and **S3**), the freely rotating *N,N* diethyl aniline donating group may have get twisted in its excited state than the rigid donor of **Cou-Rh-2** dye. Also in their open form comparatively broader absorption peaks were observed for dye **Cou-Rh-2** than dye **Cou-Rh-1** (**Fig. 5** and **S4**).

<< Please insert **Fig. 5.** Absorption (a) and emission (b) spectra of **Cou-Rh-1** in all solvents (open form) >>

<< Please insert **Table 3:** Photophysical properties of **Cou-Rh-1** dye in its open form in all solvents >>

3.2 Solvatochromism

In their spirocyclic form both **Cou-Rh-1** and **Cou-Rh-2** dyes shows red shift in their emission λ_{max} values from non-polar to polar solvents suggesting that the excited state is highly polar and is stabilized by the polar solvents very well as compared to the non-polar solvents. This observation further supported by the fact that very small variation in the absorption λ_{max} values is observed from non-polar to polar solvent suggesting that the ground state is comparatively less polar than the excited state of these dyes. **Fig. 6** represents normalized emission spectra of dye **Cou-Rh-1** in all solvents with red shift of 67 nm from non-polar to polar solvents. We correlated the solvatochromism observed in these dyes by using Lippert-Mataga equation. It is a very general equation for the effect of solvent properties such as dielectric constant and refractive index on emission λ_{max} values and does not account for specific solvent-fluorophore interactions, e.g. hydrogen bonding. The linear relationship between Stokes shift and Lippert-Mataga function for both dyes in their spirocyclic form (**Fig. 7**) suggests that solvent parameters such as dielectric constant and refractive index are collectively responsible for the red shifted emissions in polar solvents. As like other common rhodamine dyes no any red shift in their emission spectra for the open form of these dyes was observed suggesting that in their open form as like excited state ground state of these dyes is also stabilized by the polar solvents.

<< Please insert **Fig. 6.** Normalized emission spectra of **Cou-Rh-1** dye in all solvents (open form) >>

<< Please insert **Fig. 7.** Lippert-Mataga plots of dyes **Cou-Rh-1** and **Cou-Rh-2** in their spirocyclic form >>

3.3 Effect of solvent acidity and basicity on the ring opening mechanism of coumarin-rhodamine hybrid dye Cou-Rh-1

When we recorded the absorption spectra of these coumarin-rhodamine hybrid dyes in their spirocyclic as well as open form in different solvents, we found large variation in their molar extinction coefficient both in spirocyclic as well as open form. **Fig. 8** represents the absorption spectra of **Cou-Rh-1** dye in its open form in different solvent without addition of any acid. It can be seen that it preferred to remain in its open form in MeOH, acetonitrile, acetone and chloroform while in its spirocyclic form in DMF and as mixture of spirocyclic and open form in toluene and hexane. As per their observed absorbance values (if absorbance 1 is considered as 100 % conversion) in MeOH the dye preferred to remain in its open form with 75.15 % conversion and in spirocyclic form with 16.42 % which is the minimum value than any other solvent in its spirocyclic form. Similarly in DMF it preferred to remain in its spirocyclic form with 47.96 % conversion which is the highest value as compared to any other solvent and with 10.56 % it remains in its open form which is the lowest value for the dye in its open form. It is well-known that the rhodamine derivatives are stable in their spirocyclic form in neutral or basic conditions and in their open form in acidic conditions. We correlated these experimental finding

with the solvent acidity and basicity parameters proposed by Catalan [60] as well as their dielectric constants as represented in **Table 4**. As expected in methanol, a solvent with highest acidity (0.605) the dye **Cou-Rh-1** preferred to remain mostly in its open form (75.15 %) and in DMF, a solvent with highest basicity (0.613) it preferred to remain mostly in spirocyclic form (47.96 %). Similar correlation is observed in the case of other solvents such as chloroform, toluene and hexane. In acetone and acetonitrile interestingly the dye preferred to remain in open form though these solvents are very negligible acidic (0.000, 0.044) and highly basic (0.475, 0.286) in nature, may be due to their very high dielectric constants (20.7 and 37.5 respectively).

<< **Fig. 8**. Absorption spectra of **Cou-Rh-1** in different solvents in its open form in absence of TFA. >>

<< Please insert **Table 4**. Variation of absorbance/percentage of dye **Cou-Rh-1** with the variation of acidity and basicity of different solvents. >>

3.4 Interconversion of spirocyclic to open form of Cou-Rh-1 and Cou-Rh-2 dyes with the addition of TFA

Due to their unique structural properties rhodamine dyes are interconvertible into their spirocyclic and open form in the presence of acid or base. Hence we studied the interconversion mechanism of these coumarin rhodamine hybrid dyes from their spirocyclic to open form with the addition of trifluoroacetic acid in toluene (**Fig. 9** and S5). We used 10 μM solutions of **Cou-Rh-1** and **Cou-Rh-2** dyes in their spirocyclic form in toluene solvent and tested their absorption and emission spectra with the increased percentage of TFA in toluene. For both these dyes we

observed decreased absorbance of their spirocyclic form at 382 nm and 375 nm with simultaneous increased absorbance of their open form at 605 nm and 609 nm for **Cou-Rh-1** and **Cou-Rh-2** dyes respectively. Similarly with the increased percentage of TFA in toluene, we observed decreased emission intensity of their spirocyclic form at 450 and 466 nm with simultaneous increased emission intensity of their open form at 653 and 648 nm when excited at 605 and 609 nm respectively. The respective absorption and emission spectra of **Cou-Rh-1** and **Cou-Rh-2** dyes with the increased percentage of TFA in toluene are represented in **Fig. 9** and **S5** respectively. For both **Cou-Rh-1** and **Cou-Rh-2** dyes in their spirocyclic form with the increased percentage of TFA slightly red shift in their absorption λ_{\max} (10 and 4 nm) as well as emission λ_{\max} (35 and 23 nm) is observed respectively.

<< Please insert **Fig. 9**. Absorption and emission spectra of **Cou-Rh-1** with the increased percentage of TFA in toluene. >>

3.5 Effect of viscosity on absorption and emission of hybrid dyes **Cou-Rh-1** and **Cou-Rh-2**

We studied the effect of viscosity and polarity of solvents on absorption as well as emission spectra of rhodamine dyes **Cou-Rh-1** and **Cou-Rh-2** in their spirocyclic form both in absence and presence of TFA, so that their viscosity sensitivity can be tested in both visible as well as deep red region. For this purpose we choose three different mixture of solvents i.e. polar protic [EtOH-PEG 400], polar aprotic [toluene-PEG 400] and non-polar aprotic [toluene-paraffin].

(1) Mixture of polar-protic solvents [EtOH-PEG 400]

For **Cou-Rh-1** dye very high enhancement in emission intensity was observed as the percentage of PEG was increased in ethanol from 0 to 98 %, both in presence as well as absence of TFA

(10.14 and 6.41 fold respectively) (**Fig. 10**). At the same time very small variation in absorbance is observed with the increased percentage of PEG in ethanol both in presence as well as absence of TFA (**Fig. S6**). In the presence of TFA, new absorption peak at 600 nm for its open form is observed and in the absence of TFA, absorbance was decreased after the addition PEG in ethanol (**Fig. S6**). Interestingly in the presence of TFA, though the open form absorbance decreased after the addition of PEG in ethanol, the spirocyclic form absorbance is increased. Also the emission enhancement in the presence of TFA is higher as compared to that in the absence of TFA and no any enhancement of emission intensity of the open form emission peak is observed in the presence of TFA. As the spirocyclic form absorption and emission λ_{\max} mostly deals with the coumarin part, the carbonyl oxygen atom of coumarin may have protonated to initiate more effective donor-acceptor charge transfer in the presence of TFA.

<< Please insert **Fig. 10**. Emission spectra of **Cou-Rh-1** in EtOH: PEG mixture in presence (left) and absence (right) of TFA. >>

In the case of **Cou-Rh-2** dye also we studied the change in absorption as well as emission intensity with the increased percentage of PEG in ethanol in the presence or absence of TFA. If we see the absorption spectra of this dye in the presence and absence of TFA with the increased percentage of PEG in ethanol, same scenario as in **Cou-Rh-1** dye is observed (**Fig. S7**). In the emission spectra, the enhancement in emission intensity was observed with the increased percentage of PEG in ethanol both in presence and absence of TFA, but opposite to the dye **Cou-Rh-1**, it shows enhancement of emission intensity of the open form emission peak in the deep red region in the presence as well as absence of TFA. It indicates that this dye is comparatively more stable in its open form and the spirocyclic form gets easily converted into the open form

even in the presence of protic solvents such as ethanol. Both in the presence and absence of TFA almost same amount of enhancement in emission intensity was observed (4.02 and 3.98 fold respectively) (**Fig. 11**). As this dye shows good enhancement of emission intensity in its open form at above 600 nm, it can be utilized as viscosity sensor in the deep red region.

<< Please insert **Fig. 11**. Emission spectra of **Cou-Rh-2** in EtOH: PEG mixture in presence (left) and absence (right) of TFA. >>

(2) Mixture of polar-aprotic solvents [toluene-PEG 400]

In toluene-PEG mixture also as like ethanol-PEG mixture the absorption spectra of **Cou-Rh-1** and **Cou-Rh-2** dyes shows decrease in absorbance of its open form and increase in absorbance of spirocyclic form in the presence of TFA and decrease in absorbance of spirocyclic form in the absence of TFA (**Fig. S8 and S10**). In their emission spectra, **Cou-Rh-1** dye again found more stable in its spirocyclic form as compared to the **Cou-Rh-2** dye and shows emission peak only for its spirocyclic form. In the absence of TFA, for both **Cou-Rh-1** and **Cou-Rh-2** dyes quenching of emission intensity of its spirocyclic emission peak with the increased percentage of PEG in toluene was observed (**Fig. S9 and S11**). In the presence of TFA, both **Cou-Rh-1** and **Cou-Rh-2** dyes shows sudden increase in emission intensity after the addition of 30 % PEG in ethanol, but after that no much enhancement in emission intensity is observed with the increased percentage of PEG in toluene. Overall no any good emission enhancement was observed in this mixture of solvents as compared to the ethanol-PEG mixture.

(3) Mixture of non-polar-aprotic solvents [toluene-paraffin]

We also studied the absorption and emission spectra of **Cou-Rh-1** and **Cou-Rh-2** dyes in non-polar aprotic mixture of solvents i.e. toluene-paraffin in the presence of TFA. A very good enhancement in emission intensity as like EtOH-PEG mixture is observed for both the dyes, where dye **Cou-Rh-1** again showed emission enhancement in its spirocyclic form only and dye **Cou-Rh-2** showed emission enhancement in both spirocyclic as well as open form (**Fig. 12** and S12). For their spirocyclic form emission peak, comparatively higher emission enhancement of dye **Cou-Rh-1** (4.21 fold) is observed than dye **Cou-Rh-2** (2.18 fold). Dye **Cou-Rh-2** showed emission enhancement in both spirocyclic as well as open form. It showed emission enhancement of 3.56 fold for its open form at 650 nm and hence can be utilized as deep red emitting viscosity sensor. For this dye, when up to 90 % of paraffin in toluene was added highest emission intensity for the open form emission peak is observed, but after that i.e. up to 98 % of paraffin in toluene, spirocyclic form showed highest emission enhancement. In contrast to the above two solvent mixtures studied, in the toluene-paraffin mixture, absorbance of both spirocyclic and open form of both **Cou-Rh-1** and **Cou-Rh-2** dyes was decreased with the increasing percentage of paraffin in ethanol.

<< Please insert **Fig. 12**. Absorption (left) and emission (right) spectra of **Cou-Rh-1** in toluene: paraffin mixture in presence of TFA >>

In short, highest emission enhancement in EtOH-PEG mixture than toluene-paraffin mixture was observed. Hence it can be predicted that in the case of EtOH-PEG mixture both polarity as well as viscosity factors are responsible while in the case of toluene-paraffin mixture only viscosity factor is responsible for the emission enhancement and the toluene-PEG mixture is totally rejected as very low emission enhancement was observed in this mixture of solvents. Overall,

comparatively higher emission enhancement for **Cou-Rh-1** dye than **Cou-Rh-2** dye was observed, but the **Cou-Rh-1** dye can be used as viscosity sensor only in the visible region, while **Cou-Rh-2** dye can be used as viscosity sensor in both visible as well as deep red region.

3.6 Fluorescence quantum yield (Φ_f) and life time measurements

Absolute quantum yield of **Cou-Rh-1** and **Cou-Rh-2** dyes are calculated in toluene solvent in the presence and absence of TFA. Absolute quantum yield and fluorescence lifetime values are presented in **Table 5**. As we calculated the absolute quantum yield of their spirocyclic form, we found higher values in the absence of TFA which are decreased after the addition of TFA, because some amount of dye get converted into their open form also. In their spirocyclic form, dye **Cou-Rh-1** (15.1 %) shows higher quantum yield than **Cou-Rh-2** (5.8 %). At the same time, the fluorescence lifetime is higher for **Cou-Rh-2** dye (4.97 ns) than **Cou-Rh-1** dye (2.07 ns). Fluorescence Lifetime bi-exponential curves indicate the existence of two species at the equilibrium may be due to the mixture of their spirocyclic and open form (**Fig. 13**). We also studied the lifetime measurement of **Cou-Rh-1** dye in different viscosity mixture of solvents and it is found that as the ratio of PEG 400 increases i.e. viscosity increases lifetime is also increases (**Table 6**). The lifetime measured in toluene solvent was 0.85 ns and it was increased up to 1.93 ns for toluene-PEG (2:98) mixture.

<< Please insert **Table 5**. Fluorescence quantum yield and life time measurements of dyes **Cou-Rh-1** and **Cou-Rh-2** >>

<< Please insert **Table 6**. Lifetime measurement of **Cou-Rh-1** dye in different composition of PEG 400 in toluene >>

<< Please insert **Fig. 13** Lifetime measurement spectra of **Cou-Rh-1** (a) and **Cou-Rh-2** (b) in THF and toluene respectively. >>

3.7 Photo stability study of **Cou-Rh-1** for its spirocyclic and open form

Photo stability study of dye **Cou-Rh-1** both for its spirocyclic as well as open form was carried out at various time intervals under UV light. For this purpose their 5 μM solutions in toluene solvent were irradiated at 254 nm up to 150 min. The absorption and emission spectra of this dye, both in spirocyclic as well as open form were recorded at each 30 min. time interval. **Fig. 14** represents the absorption and emission spectra of **Cou-Rh-1** dye for its spirocyclic form at each 30 min time interval, while **Fig. S13** represents the absorption and emission spectra of this dye for its open form at each 30 min. time interval. Emission spectra of **Cou-Rh-1** were recorded by exciting at 375 nm for its spirocyclic form and at 588 nm for its open form. We found this dye highly photo stable both in its spirocyclic as well as open form under UV light, as no remarkable change in its absorbance as well as emission intensity for both the forms was observed.

<<Please insert **Fig. 14**. Absorption (a) and emission (b) spectra of dye **Cou-Rh-1** (spirocyclic form) after the irradiation of UV light (254 nm) at different time intervals in toluene solvent (λ_{ex} : 375 nm). >>

3.8 Optimized structures of **Cou-Rh-1** and **Cou-Rh-2** dyes in their spirocyclic and open form by DFT method

To correlate our experimental finding theoretically we optimized the structures of **Cou-Rh-1** and **Cou-Rh-2** dyes in their spirocyclic and open form using Density Functional Theory (DFT)[51] with Gaussian 09 package and the popular hybrid functional B3LYP. The basis set used was 6-

31G (d) in both DFT and time-dependent density functional theory (TD-DFT) method. The computationally derived vertical excitation energies and oscillator strengths of these dyes were obtained for the lowest 10 singlet-singlet transitions using TD-DFT method at the same hybrid functional and basis set [54]. **Fig. 15** represents the frontier molecular orbital profile of **Cou-Rh-1** and **Cou-Rh-2** dyes in their spirocyclic and open form displaying electronic distributions in their HOMO and LUMO energy levels in toluene and chloroform solvent respectively.

<< Please insert **Fig. 15**. HOMO-LUMO FMO diagrams of **Cou-Rh-1** and **Cou-Rh-2** dyes in their spirocyclic and open form in toluene and chloroform solvent respectively at ground state.

>>

In their spirocyclic form, for **Cou-Rh-1** dye electronic density at HOMO level is situated on coumarin side triphenylamine donor while for **Cou-Rh-2** dye it is situated on rhodamine side julolidine donor highlighting different donating ability of *N,N* diethyl aniline and julolidine donor. At LUMO level for both the dyes in their spirocyclic form most of the electron density is situated on lactone ring of rhodamine and some part is spread towards coumarin core. In their open form at HOMO level for both the dyes the electron density is situated at central coumarin fused xanthene core while at LUMO level it is mostly situated on carboxyl group substituted phenyl ring of rhodamine and no any overlap of electron densities between HOMO and LUMO energy level is observed. As complete charge transfer is observed for these dyes in their open form as compared to the partial charge transfer observed in their spirocyclic form, good interaction between the donor and acceptor is expected in the open form of these dyes.

We also calculated the energy difference between HOMO and LUMO energy levels for both **Cou-Rh-1** and **Cou-Rh-2** dyes in their both spirocyclic as well as open form. In general lower

energy difference is observed in their open form (2.37 and 2.14 eV) as compared to their respective spirocyclic form (3.67 and 3.58 eV). Also in between **Cou-Rh-1** and **Cou-Rh-2**, the dye with better donating group i.e. **Cou-Rh-2** shows comparatively lower energy difference between HOMO and LUMO than **Cou-Rh-1**. When we go from spirocyclic to open form, energies of HOMO level are increased rather than decreasing the energies of LUMO level. The HOMO-LUMO energy diagrams of **Cou-Rh-1** and **Cou-Rh-2** in their spirocyclic and open form is represented in **Fig. 16**. We compared the experimental absorption λ_{\max} values with the computationally derived vertical excitations and a minimum deviation between them in their spirocyclic as well as open form is observed (**Table 7**). We also compared the experimentally calculated and computationally derived oscillator strength (f) values and the computationally derived values are lower than the respective experimental one in both spirocyclic as well as open form.

<< Please insert **Fig. 16**. HOMO-LUMO energy diagrams of **Cou-Rh-1** and **Cou-Rh-2** dyes in their spirocyclic and open form chloroform solvent. >>

<< Please insert **Table 7**. Comparative experimental and computational photophysical parameters of **Cou-Rh-1** and **Cou-Rh-2** dyes in their spirocyclic (toluene) and open form (chloroform). >>

4 Conclusion

By using H-NMP.HSO₄ as novel reaction media for the synthesis of rhodamine core we synthesized two novel triphenylamine based coumarin-rhodamine hybrid derivatives. A detail photophysical study of these dyes in their spirocyclic and open form is presented in a comparative approach. We found red shifted absorption and emission peaks for these dyes in

their open form than the reported **RH-B** and **RH-101** dyes with comparatively higher Stokes shift also. We calculated the presence of spirocyclic and open form of **Cou-Rh-1** dye in different solvents and are correlated with the acidity or basicity as well as dielectric constant of the respective solvent. The ring opening mechanism of both the dyes from spirocyclic to open form is also presented with the addition of TFA in toluene. Viscosity sensitivity of these dyes was studied in different mixture of solvents and both the dyes are found to show very good emission enhancement in protic-polar mixture of solvents (EtOH-PEG) after increasing the ratio of polyethylene glycol (PEG) in ethanol. Similar enhancement in emission intensity in aprotic-non-polar mixture of solvent (toluene-paraffin) was also observed but the former was showing better results. Hence it can be concluded that when polarity and viscosity works together better results were obtained than when only viscosity works independently. As viscosity sensitivity of these dyes was studied in both spirocyclic and open form they can be used as viscosity sensors in the visible as well as deep red region. We also found better support to our experimental observations with the computationally obtained results.

Acknowledgements

Shantaram Kothavale and Amol Jadhav are grateful to UGC for research support under UGC-SRF fellowship. We are also thankful to the Sophisticated Analytical Instrument Facility (SAIF), IIT, Mumbai, India for the recording of mass and HR-MS spectra.

References

- [1] Recommendation for a selected method for the measurement of plasma viscosity. International Committee for Standardization in Haematology. *J Clin Pathol* 1984;37:1147–52.

- [2] Wang S, Boss AH, Kensey KR, Rosenson RS. Variations of whole blood viscosity using RheologTM—a new scanning capillary viscometer. *Clin Chim Acta* 2003;332:79–82. doi:http://dx.doi.org/10.1016/S0009-8981(03)00125-6.
- [3] Haidekker M a, Theodorakis E a. Molecular rotors--fluorescent biosensors for viscosity and flow. *Org Biomol Chem* 2007;5:1669–78. doi:10.1039/b618415d.
- [4] Geddes CD. 1 and 2-Photon Fluorescence Anisotropy Decay to Probe the Kinetic and Structural Evolution of Sol-Gel Glasses: A Summary. *J Fluoresc* 2002;12:343–67. doi:10.1023/A:1021353707955.
- [5] Dragan A, Graham AE, Geddes CD. Fluorescence-based Broad Dynamic Range Viscosity Probes. *J Fluoresc* 2014;24:397–402. doi:10.1007/s10895-013-1304-9.
- [6] Grabowski ZR, Rotkiewicz K, Rettig W. Structural Changes Accompanying Intramolecular Electron Transfer: Focus on Twisted Intramolecular Charge-Transfer States and Structures. *Chem Rev* 2003;103:3899–4032. doi:10.1021/cr9407451.
- [7] Haidekker M a, Theodorakis E a. Environment-sensitive behavior of fluorescent molecular rotors. *J Biol Eng* 2010;4:11. doi:10.1186/1754-1611-4-11.
- [8] Loutfy RO, Arnold BA. Effect of viscosity and temperature on torsional relaxation of molecular rotors. *J Phys Chem* 1982;86. doi:10.1021/j100218a023.
- [9] Safarzadeh-Amiri A. Solvent and temperature effects on the decay dynamics of [p-N,N-(dialkylamino)benzylidene]malononitriles. *Chem Phys Lett* 1986;129:225–30. doi:http://dx.doi.org/10.1016/0009-2614(86)80201-9.
- [10] Blanchard-Desce M, Wortmann R, Lebus S, Lehn J-M, Krämer P. Intramolecular charge transfer in elongated donor-acceptor conjugated polyenes. *Chem Phys Lett* 1995;243:526–32. doi:http://dx.doi.org/10.1016/0009-2614(95)00895-B.
- [11] Allen BD, Benniston AC, Harriman A, Rostron SA, Yu C. The photophysical properties of a julolidene-based molecular rotor. *Phys Chem Chem Phys* 2005;7. doi:10.1039/b507165h.
- [12] Zhu L-L, Qu D-H, Zhang D, Chen Z-F, Wang Q-C, Tian H. Dual-mode tunable viscosity sensitivity of a rotor-based fluorescent dye. *Tetrahedron* 2010;66:1254–60. doi:http://dx.doi.org/10.1016/j.tet.2009.12.014.
- [13] Yoon H.J, Dakanali M, Lichlyter D, Chang WM, Nguyen KA, Nipper ME, et al. Synthesis and evaluation of self-calibrating ratiometric viscosity sensors. *Org Biomol Chem* 2011;9:3530–40. doi:10.1039/C0OB01042A.

- [14] Alamiry M, Bahaidarah E, Harriman A, Bura T, Ziessel R. Fluorescent molecular rotors under pressure: synergistic effects of an inert polymer. *RSC Adv* 2012;2:9851–9. doi:10.1039/C2RA20786A.
- [15] Kuimova M, Yahioglu G, Levitt JA, Suhling K. Molecular rotor measures viscosity of live cells via fluorescence lifetime imaging. *J Am Chem Soc* 2008;130. doi:10.1021/ja800570d.
- [16] Marfin YS, Merkushev D, Levshanov GA, Rumyantsev E V. Fluorescent Properties of 8-phenylBODIPY in Ethanol – Ethylene Glycol Mixed Solutions. *J Fluoresc* 2014;24:1613–9. doi:10.1007/s10895-014-1447-3.
- [17] Yin X, Li Y, Zhu Y, Jing X, Li Y, Zhu D. A highly sensitive viscosity probe based on ferrocene-BODIPY dyads. *Dalt Trans* 2010;39:9929–35. doi:10.1039/C0DT00309C.
- [18] De Silva AP, Gunaratne HQN, Gunnlaugsson T, Huxley AJM, McCoy CP, Rademacher JT, et al. Signaling Recognition Events with Fluorescent Sensors and Switches. *Chem Rev* 1997;97:1515–66. doi:10.1021/cr960386p.
- [19] Nolan EM, Lippard SJ. Tools and Tactics for the Optical Detection of Mercuric Ion. *Chem Rev* 2008;108:3443–80. doi:10.1021/cr068000q.
- [20] Waggoner A. Fluorescent labels for proteomics and genomics. *Curr Opin Chem Biol* 2006;10:62–6. doi:http://dx.doi.org/10.1016/j.cbpa.2006.01.005.
- [21] Resch-Genger U, Grabolle M, Cavaliere-Jaricot S, Nitschke R, Nann T. Quantum dots versus organic dyes as fluorescent labels. *Nat Meth* 2008;5:763–75.
- [22] Gonçalves MST. Fluorescent Labeling of Biomolecules with Organic Probes. *Chem Rev* 2009;109:190–212. doi:10.1021/cr0783840.
- [23] Szaciłowski K. Digital Information Processing in Molecular Systems. *Chem Rev* 2008;108:3481–548. doi:10.1021/cr068403q.
- [24] Straight SD, Liddell PA, Terazono Y, Moore TA, Moore AL, Gust D. All-Photonic Molecular XOR and NOR Logic Gates Based on Photochemical Control of Fluorescence in a Fulgimide–Porphyrin–Dithienylethene Triad. *Adv Funct Mater* 2007;17:777–85. doi:10.1002/adfm.200600802.
- [25] Chen C-T. Evolution of Red Organic Light-Emitting Diodes: Materials and Devices. *Chem Mater* 2004;16:4389–400. doi:10.1021/cm049679m.
- [26] Li ZH, Wong MS. Synthesis and Functional Properties of End-Dendronized Oligo(9,9-diphenyl)fluorenes. *Org Lett* 2006;8:1499–502. doi:10.1021/ol0604062.

- [27] Domercq B, Grasso C, Maldonado J-L, Halik M, Barlow S, Marder SR, et al. Electron-Transport Properties and Use in Organic Light-Emitting Diodes of a Bis(dioxaborine)fluorene Derivative. *J Phys Chem B* 2004;108:8647–51. doi:10.1021/jp036779r.
- [28] Li B, Li J, Fu Y, Bo Z. Porphyrins with Four Monodisperse Oligofluorene Arms as Efficient Red Light-Emitting Materials. *J Am Chem Soc* 2004;126:3430–1. doi:10.1021/ja039832y.
- [29] Zhang X, Chen Z-K, Loh KP. Coordination-Assisted Assembly of 1-D Nanostructured Light-Harvesting Antenna. *J Am Chem Soc* 2009;131:7210–1. doi:10.1021/ja901041d.
- [30] Zrig S, Rémy P, Andrioletti B, Rose E, Asselberghs I, Clays K. Engineering Tuneable Light-Harvesting Systems with Oligothiophene Donors and Mono- or Bis-Bodipy Acceptors. *J Org Chem* 2008;73:1563–6. doi:10.1021/jo702066v.
- [31] Tyson DS, Castellano FN. Light-Harvesting Arrays with Coumarin Donors and MLCT Acceptors. *Inorg Chem* 1999;38:4382–3. doi:10.1021/ic9905300.
- [32] Becker K, Lupton JM. Efficient Light Harvesting in Dye-Endcapped Conjugated Polymers Probed by Single Molecule Spectroscopy. *J Am Chem Soc* 2006;128:6468–79. doi:10.1021/ja0609405.
- [33] Zhang X, Xiao Y, Qian X. A Ratiometric Fluorescent Probe Based on FRET for Imaging Hg²⁺ Ions in Living Cells. *Angew Chemie Int Ed* 2008;47:8025–9. doi:10.1002/anie.200803246.
- [34] Thorne A. An Introduction to Laser Spectroscopy. *Meas Sci Technol* 2009;7:1–2. doi:10.1088/0957-0233/7/11/022.
- [35] Ogawa M, Kosaka N, Choyke PL, Kobayashi H. <http://www.w3.org/1999/xhtml> In vivo Molecular Imaging of Cancer with a Quenching Near-Infrared Fluorescent Probe Using Conjugates of Monoclonal Antibodies and Indocyanine Green; *Cancer Res* 2009;69:1268 LP – 1272.
- [36] Sheth RA, Tam JM, Maricevich MA, Josephson L, Mahmood U. Quantitative endovascular fluorescence-based molecular imaging through blood of arterial wall inflammation. *Radiology* 2009;251:813–21. doi:10.1148/radiol.2513081450.
- [37] Quang DT, Kim JS. Fluoro- and Chromogenic Chemodosimeters for Heavy Metal Ion Detection in Solution and Biospecimens. *Chem Rev* 2010;110:6280–301. doi:10.1021/cr100154p.

- [38] Kim HN, Lee MH, Kim HJ, Kim JS, Yoon J. A new trend in rhodamine-based chemosensors: application of spirolactam ring-opening to sensing ions. *Chem Soc Rev* 2008;37:1465–72. doi:10.1039/B802497A.
- [39] Beija M, Afonso CAM, Martinho JMG. Synthesis and applications of Rhodamine derivatives as fluorescent probes. *Chem Soc Rev* 2009;38:2410–33. doi:10.1039/B901612K.
- [40] Detty MR, Prasad PN, Donnelly DJ, Ohulchanskyy T, Gibson SL, Hilf R. Synthesis, properties, and photodynamic properties in vitro of heavy-chalcogen analogues of tetramethylrosamine. *Bioorg Med Chem* 2004;12:2537–44. doi:http://dx.doi.org/10.1016/j.bmc.2004.03.029.
- [41] Lieberwirth U, Arden-Jacob J, Drexhage KH, Herten DP, Müller R, Neumann M, et al. Multiplex Dye DNA Sequencing in Capillary Gel Electrophoresis by Diode Laser-Based Time-Resolved Fluorescence Detection. *Anal Chem* 1998;70:4771–9. doi:10.1021/ac980230k.
- [42] Yang P, Zhao J, Wu W, Yu X, Liu Y. Accessing the Long-Lived Triplet Excited States in Bodipy-Conjugated 2-(2-Hydroxyphenyl) Benzothiazole/Benzoxazoles and Applications as Organic Triplet Photosensitizers for Photooxidations. *J Org Chem* 2012;77:6166–78. doi:10.1021/jo300943t.
- [43] Houari Y, Chibani S, Jacquemin D, Laurent AD. TD-DFT Assessment of the Excited State Intramolecular Proton Transfer in Hydroxyphenylbenzimidazole (HBI) Dyes. *J Phys Chem B* 2015;119:2180–92. doi:10.1021/jp505036d.
- [44] Xie L, Chen Y, Wu W, Guo H, Zhao J, Yu X. Fluorescent coumarin derivatives with large stokes shift, dual emission and solid state luminescent properties: An experimental and theoretical study. *Dye Pigment* 2012;92:1361–9. doi:10.1016/j.dyepig.2011.09.023.
- [45] Barman S, Mukhopadhyay SK, Gangopadhyay M, Biswas S, Dey S, Singh NDP. Coumarin-benzothiazole-chlorambucil (Cou-Benz-Cbl) conjugate: an ESIPT based pH sensitive photoresponsive drug delivery system. *J Mater Chem B* 2015;3:3490–7. doi:10.1039/C4TB02081B.
- [46] Bochkov AY, Akchurin IO, Dyachenko OA, Traven VF. NIR-fluorescent coumarin-fused BODIPY dyes with large Stokes shifts. *Chem Commun* 2013;49:11653–5. doi:10.1039/C3CC46498A.
- [47] Esnal I, Duran-Sampedro G, Agarrabeitia AR, Banuelos J, Garcia-Moreno I, Macias MA, et al. Coumarin-BODIPY hybrids by heteroatom linkage: versatile, tunable and photostable dye lasers for UV irradiation. *Phys Chem Chem Phys* 2015;17:8239–47. doi:10.1039/C5CP00193E.

- [48] Yu H, Jin L, Dai Y, Li H, Xiao Y. From a BODIPY-rhodamine scaffold to a ratiometric fluorescent probe for nitric oxide. *New J Chem* 2013;37:1688–91. doi:10.1039/C3NJ41127C.
- [49] Karakus E, Ucuncu M, Emrullahoglu M. A rhodamine/BODIPY-based fluorescent probe for the differential detection of Hg(ii) and Au(iii). *Chem Commun* 2014;50:1119–21. doi:10.1039/C3CC48436J.
- [50] Chen J, Liu W, Zhou B, Niu G, Zhang H, Wu J, et al. Coumarin- and rhodamine-fused deep red fluorescent dyes: Synthesis, photophysical properties, and bioimaging in vitro. *J Org Chem* 2013;78:6121–30. doi:10.1021/jo400783x.
- [51] Kohn W, Sham LJ. Self-Consistent Equations Including Exchange and Correlation Effects. *Phys Rev* 1965;140:A1133–8. doi:10.1103/PhysRev.140.A1133.
- [52] Becke A. A new mixing of Hartree–Fock and local density-functional theories. *J Chem Phys* 1993;98:1372. doi:10.1063/1.464304.
- [53] Lee C, Yang W, Parr RG. Development of the Colle-Salvetti correlation-energy formula into a functional of the electron density. *Phys Rev B* 1988;37:785–9. doi:10.1103/PhysRevB.37.785.
- [54] Scalmani G, Frisch M, Mennucci B, Tomasi J, Cammi R, Barone V. Geometries and properties of excited states in the gas phase and in solution. *J Chem Phys* 2006;124:94107. doi:10.1063/1.2173258.
- [55] Varga M, Kapui Z, Bátori S, Nagy LT, Vasvári-Debreczy L, Mikus E, et al. A novel orally active inhibitor of HLE. *Eur J Med Chem* 2003;38:421–5. doi:10.1016/S0223-5234(03)00046-1.
- [56] Kamino S, Horio Y, Komeda S, Minoura K, Ichikawa H, Horigome J, et al. A new class of rhodamine luminophores: design, syntheses and aggregation-induced emission enhancement. *Chem Commun* 2010;46:9013–5. doi:10.1039/C0CC03407J.
- [57] Homma M, Takei Y, Murata A, Inoue T, Takeoka S. A ratiometric fluorescent molecular probe for visualization of mitochondrial temperature in living cells. *Chem Commun* 2015;51:6194–7. doi:10.1039/C4CC10349A.
- [58] Kothavale S, Sekar N. Methoxy supported, deep red emitting mono, bis and tris triphenylamine-isophorone based styryl colorants: Synthesis, photophysical properties, ICT, TICT emission and viscosity sensitivity. *Dye Pigment* 2017;136:116–30. doi:http://dx.doi.org/10.1016/j.dyepig.2016.08.025.
- [59] Kothavale S, Sekar N. Novel pyrazino-phenanthroline based rigid donor- π -acceptor compounds: A detail study of optical properties, acidochromism, solvatochromism and

structure-property relationship. Dye Pigment 2017;136:31–45.
doi:<http://dx.doi.org/10.1016/j.dyepig.2016.08.032>.

- [60] Catalán J. Toward a Generalized Treatment of the Solvent Effect Based on Four Empirical Scales: Dipolarity (SdP, a New Scale), Polarizability (SP), Acidity (SA), and Basicity (SB) of the Medium. *J Phys Chem B* 2009;113:5951–60. doi:10.1021/jp8095727.

Tables**Table 1.** Photophysical properties of **Cou-Rh-1** and **Cou-Rh-2** in their spirocyclic and open form

Solvent	λ_{abs} (nm)	$\epsilon_{\text{max}} \times 10^4$ ($\text{M}^{-1} \text{cm}^{-1}$)	fwhm (nm)	λ_{ems} (nm)	Stokes shift (nm) (cm ⁻¹)		f	μ_{eg} (debye)
Cou-Rh-1 cyclic	371	3.81	46	430	59	3698	0.63	7.04
Cou-Rh-2 cyclic	371	2.99	51	435	64	3966	0.59	6.81
Cou-Rh-1 open	610	8.91	73	678	68	1644	0.90	10.84
Cou-Rh-2 open	614	5.09	85	668	54	1316	0.62	9.00

Table 2. Photophysical properties of **Cou-Rh-1** dye in its spirocyclic form in all solvents

Solvent	λ_{abs} (nm)	$\epsilon_{\text{max}} \times 10^4$ ($\text{M}^{-1} \text{cm}^{-1}$)	fwhm (nm)	λ_{ems} (nm)	Stokes shift (nm) (cm ⁻¹)		f	μ_{eg} (debye)
Hexane	371	3.81	46	430	59	3698	0.63	7.04
Toluene	376	3.47	47	454	78	4569	0.59	6.89
Chloroform	378	3.87	44	462	84	4810	0.68	7.42
Acetone	372	3.82	50	497	125	6761	0.61	6.97
MeOH	377	4.02	48	460	83	4786	0.73	7.64
Acetonitrile	372	4.38	51	421	49	3133	0.81	8.00
DMSO	375	4.04	48	476	101	5661	0.75	7.74

Table 3. Photophysical properties of **Cou-Rh-1** dye in its open form in all solvents

Solvent	λ_{abs} (nm)	$\epsilon_{\text{max}} \times 10^4$ ($\text{M}^{-1} \text{cm}^{-1}$)	fwhm (nm)	λ_{ems} (nm)	Stokes shift (nm) (cm ⁻¹)		f	μ_{eg} (debye)
Hexane	601	8.07	73	664	63	1577	0.83	10.31
Toluene	607	7.57	74	669	62	1523	0.77	9.99

Chloroform	610	8.91	73	678	68	1644	0.90	10.84
Acetone	592	7.88	76	641	49	1288	0.83	10.23
MeOH	589	8.14	74	645	56	1472	0.85	10.34
Acetonitrile	592	7.43	77	648	56	1459	0.85	10.37
DMSO	596	0.44	85	648	52	1346	0.05	2.61

Table 4. Variation of absorbance/percentage of dye **Cou-Rh-1** with the variation of acidity and basicity of different solvents.

Solvent	Dielectric constant	Solvent acidity	Solvent basicity	Cyclic form percentage	Open form percentage
Hexane	1.89	0.000	0.056	31.61	25.19
Toluene	2.38	0.000	0.128	38.43	33.09
Chloroform	4.81	0.047	0.071	27.49	49.61
Acetone	20.7	0.000	0.475	23.51	56.43
MeOH	32.7	0.605	0.545	16.42	75.15
Acetonitrile	37.5	0.044	0.286	18.91	67.82
DMF	36.7	0.031	0.613	47.96	10.56

Table 5. Fluorescence quantum yield and life time measurements of dyes **Cou-Rh-1** and **Cou-Rh-2**.

Molecules (Solvents)	Excitation wavelength (nm)	Avg. QY (%)	Standard-deviation σ	χ^2	Life Time $\tau_{[int]}$ [ns]
Cou-Rh-1 (Toluene)	377	15.1	0.1	1.268	2.078
Cou-Rh-1 (Toluene+TFA)	377	1.9	0.13	-	-
Cou-Rh-2 (Toluene)	375	5.8	0.2	1.181	4.973
Cou-Rh-2 (Toluene+TFA)	375	5.2	0.05	-	-

Table 6. Lifetime measurement of **Cou-Rh-1** dye in different composition of PEG 400 in toluene

Toluene: PEG mixture (%)	B_i	τ_i	B_i	τ_i	B_i	τ_i	$\tau_{[int]}$	χ^2
		[ns]		[ns]		[ns]	[ns]	
Toluene (100)	0.0070	0.019	0.0119	0.710	0.0002	2.961	0.857	1.112
Toluene:PEG (70:30)	0.0081	0.012	0.0111	0.825	0.0002	3.297	0.991	1.136
Toluene:PEG (50:50)	-0.0050	0.323	0.0132	0.902	0.0006	2.382	1.061	1.007
Toluene:PEG (20:80)	-0.0028	0.281	0.010300	1.435	0.0003	3.868	1.612	1.053
Toluene:PEG (10:90)	-0.0332	0.015	0.0090	1.689	0.0003	4.101	1.870	1.054
Toluene:PEG (2:98)	-0.0016	0.268	0.0075	1.651	0.002	2.617	1.938	0.981

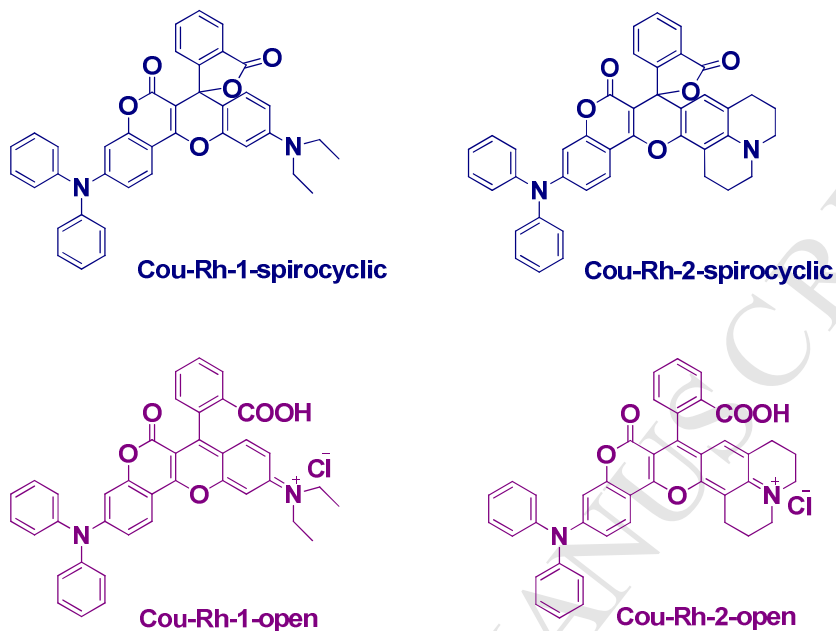
Table 7. Comparative experimental and computational photophysical parameters of **Cou-Rh-1** and **Cou-Rh-2** dyes in their spirocyclic (toluene) and open form (chloroform).

Dye	<u>Experimental/Computational (cyclic form)</u>					<u>Experimental/Computational (open form)</u>				
	λ_{abs}^a	λ_{abs}^b	f^c	f^d	Major ^e	λ_{abs}^f	λ_{abs}^g	f^h	f^i	Major ^j
	(nm)	(nm)			Contribution	(nm)	(nm)			Contribution
Cou-Rh-1	371	385	0.34	0.7946	H → L (98%)	607	608	0.20	0.0137	H → L+1 (98%)
Cou-Rh-2	371	400	0.29	0.1694	H → L (98%)	614	688	0.22	0.0155	H → L+1 (98%)

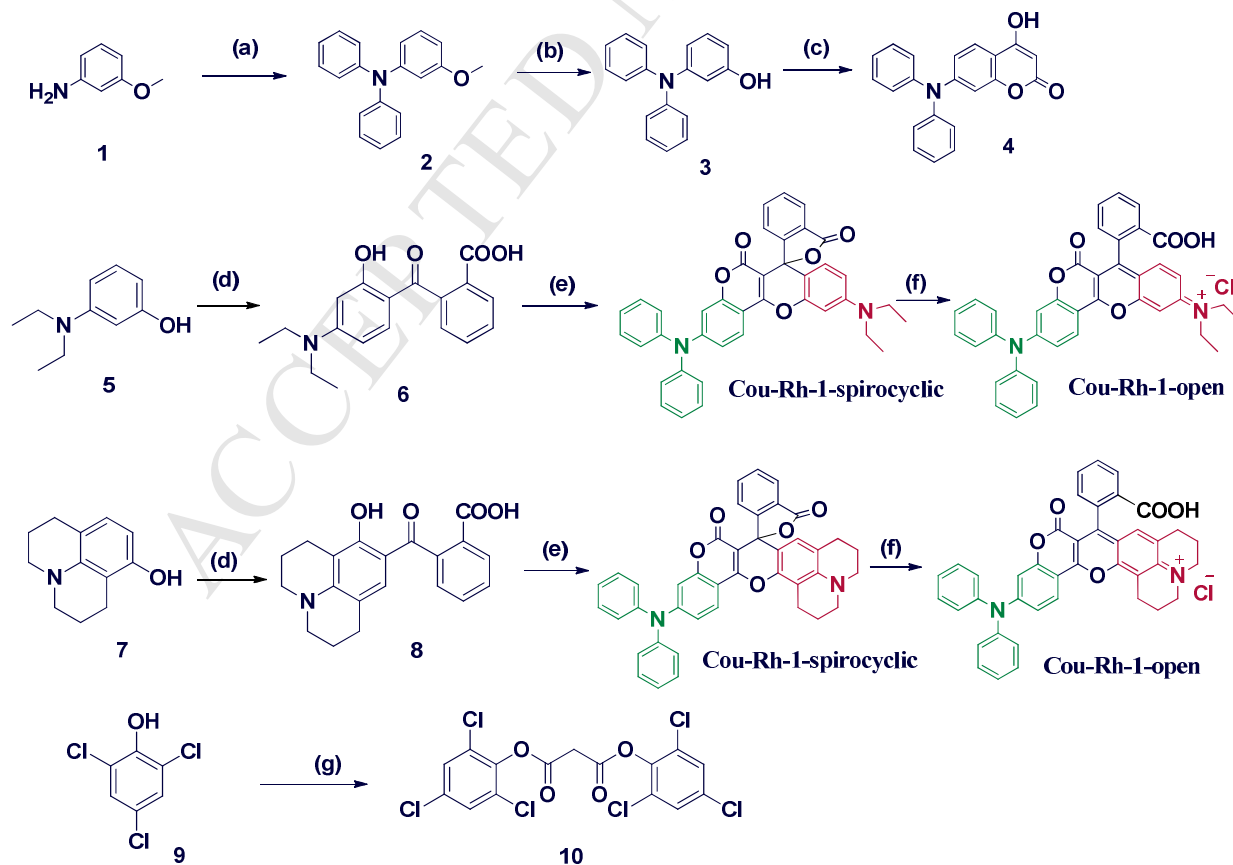
^aExperimental absorption λ_{max} of close form, ^bComputational vertical excitation, ^cExperimentally calculated oscillator strength, ^dTheoretical oscillator strength, ^eMajor electronic transition from ground to excited state, ^fExperimental absorption λ_{max} of open form, ^gComputational absorption λ_{max} , ^hOscillator strength of vertical excitation, ⁱTheoretical oscillator strength, ^jMajor electronic transition from excited state to ground state.

Figures

Fig. 1 Structure of the coumarin-rhodamine hybrid dyes **Cou-Rh-1** and **Cou-Rh-2**



Scheme 1: Synthesis of coumarin-rhodamine hybrids **Cou-Rh-1** and **Cou-Rh-2**



(a) Iodobenzene, *p*-t-butoxide, 1, 10-phenanthroline/CuI, toluene, N₂ atmosphere (b) pyridine, HCl, 200 ° C, overnight (c) Intermediate 10, toluene, reflux, overnight, N₂ atmosphere (d) Phthalic anhydride, toluene, reflux, overnight, N₂ atmosphere, (e) Intermediate 4, NMP.HSO₄, 90 ° C, overnight, (f) MeOH.HCl, R.T. 1 hr. (g) malonic acid, POCl₃, reflux, overnight.

Fig. 2: Normalized absorption and emission spectra of dyes **Cou-Rh-1** and **Cou-Rh-2** in their open form

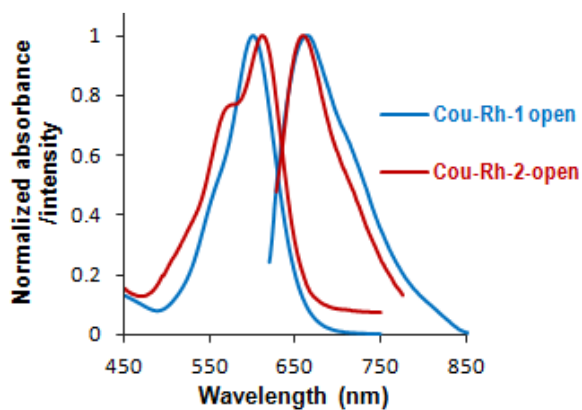


Fig. 3: Normalized absorption and emission spectra of **RH-B**, **RH-101**, **Cou-Rh-1** and **Cou-Rh-2** in their open form in chloroform solvent

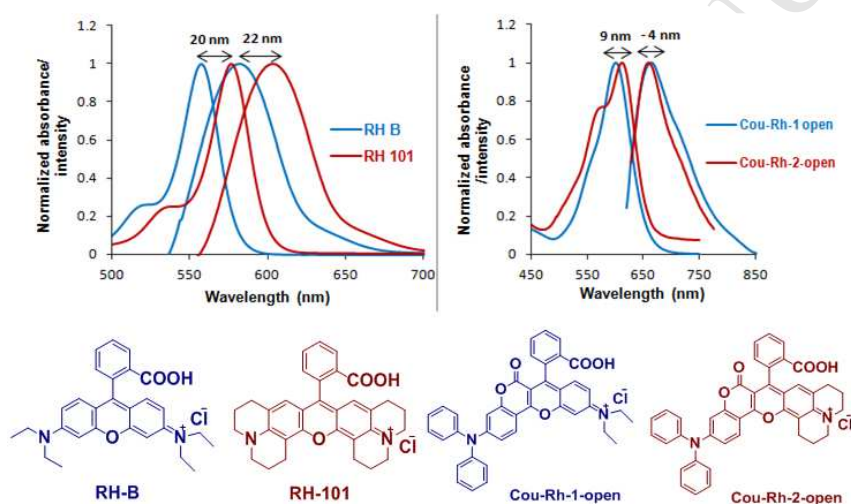


Fig. 4: Absorption (a) and emission (b) spectra of **Cou-Rh-1** in different solvents in their spirocyclic form.

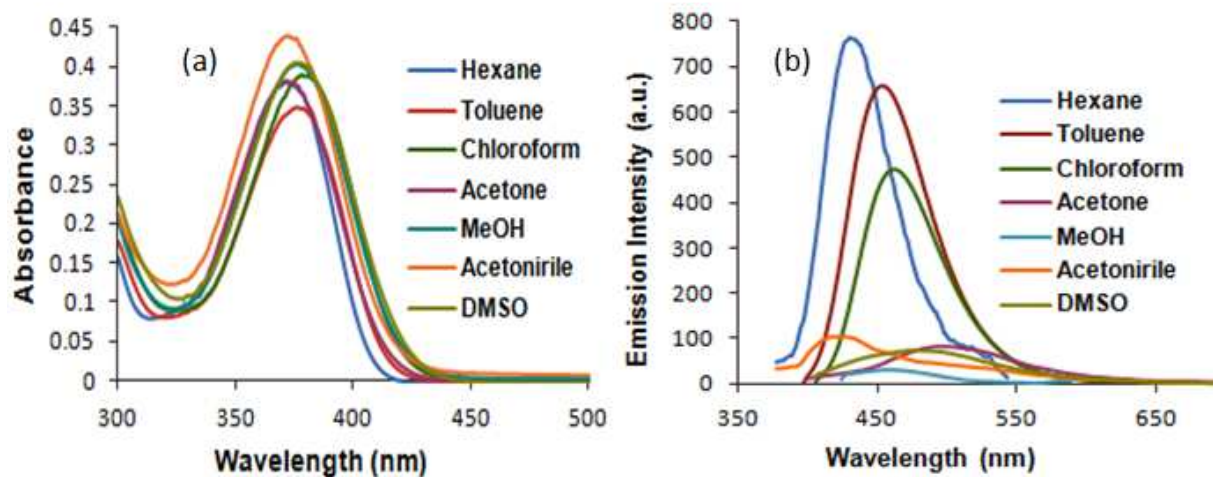


Fig. 5. Absorption (a) and emission (b) spectra of **Cou-Rh-1** in all solvents (open form)

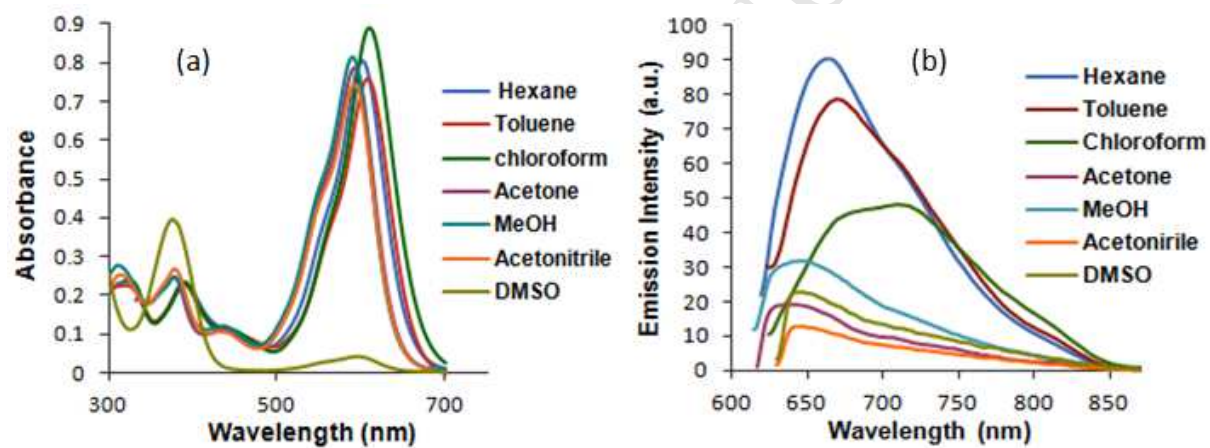


Fig. 6. Normalized emission spectra of **Cou-Rh-1** dye in all solvents (open form)

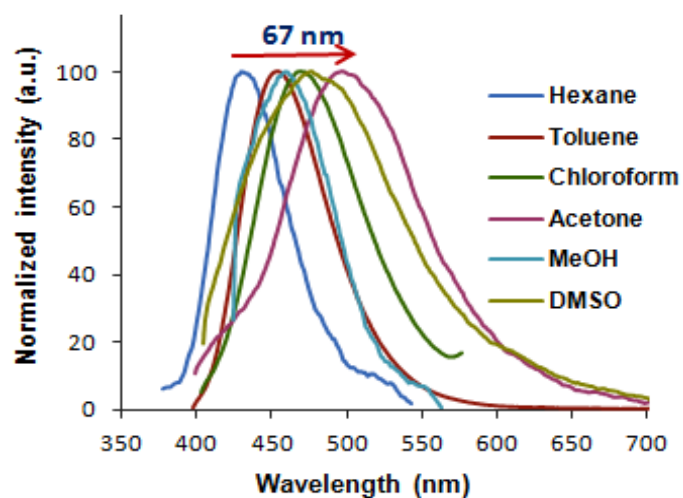


Fig. 7. Lippert-Mataga plots of dyes **Cou-Rh-1** and **Cou-Rh-2** in their spirocyclic form

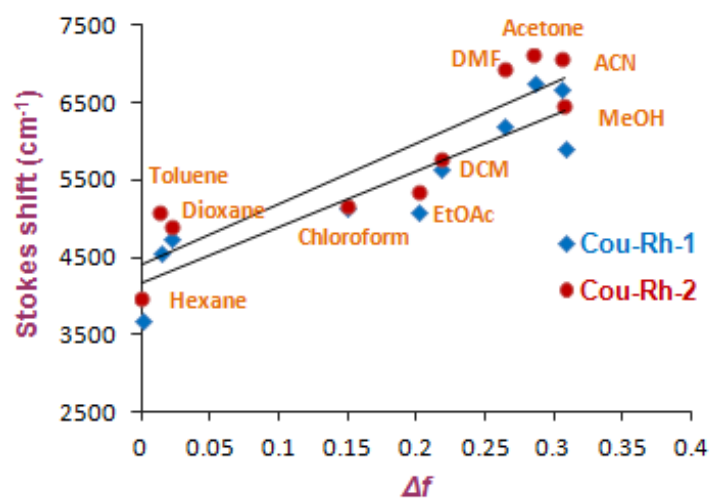


Fig. 8. Absorption spectra of **Cou-Rh-1** in different solvents in its open form in absence of TFA.

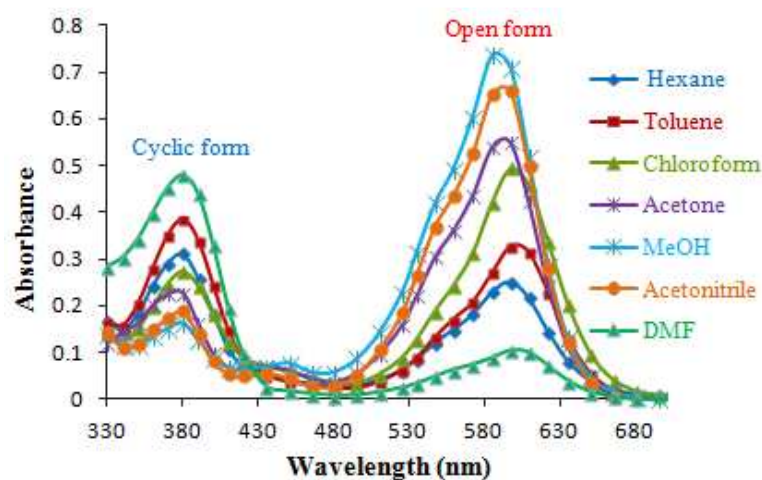


Fig. 9. Absorption and emission spectra of **Cou-Rh-1** with the increased percentage of TFA in toluene.

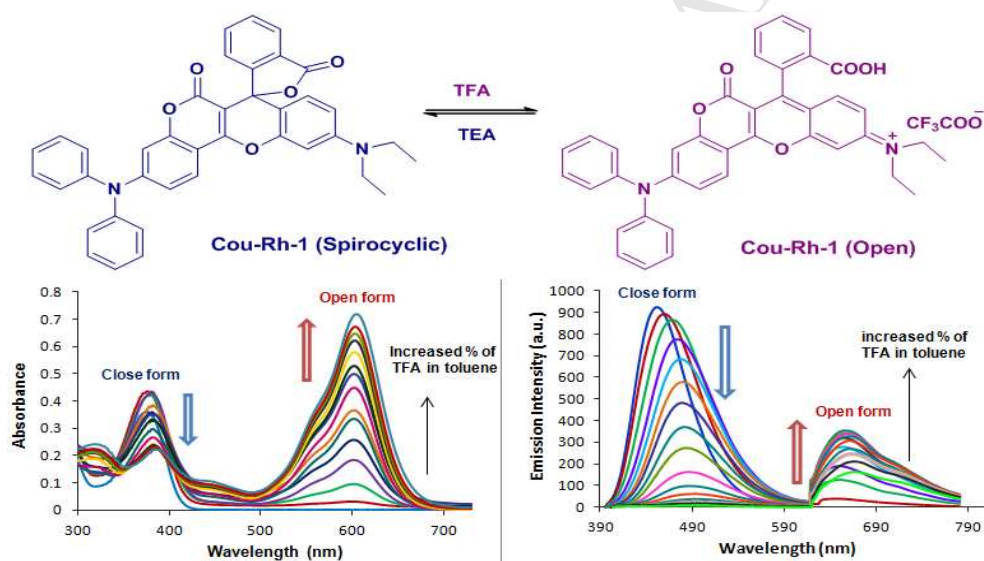


Fig. 10 Emission spectra of **Cou-Rh-1** in EtOH: PEG mixture in presence (left) and absence (right) of TFA.

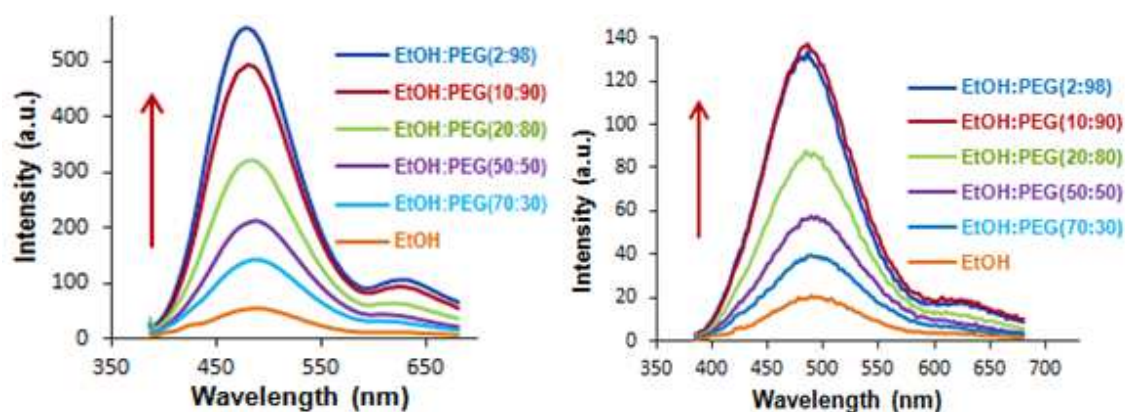


Fig. 11 Emission spectra of **Cou-Rh-2** in EtOH: PEG mixture in presence (left) and absence (right) of TFA.

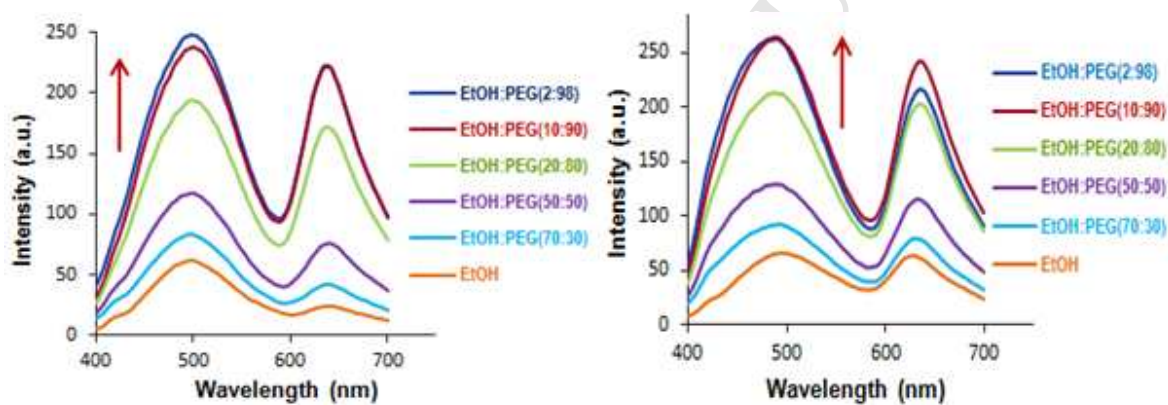


Fig. 12 Absorption (left) and emission (right) spectra of **Cou-Rh-1** in toluene: paraffin mixture in presence of TFA

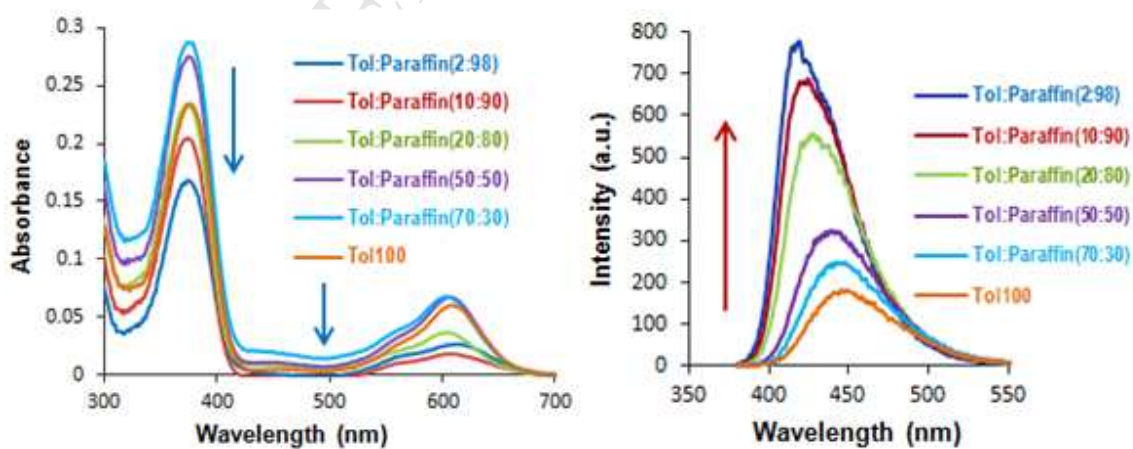


Fig. 13 Lifetime measurement spectra of **Cou-Rh-1** (a) and **Cou-Rh-2** (b) in THF and toluene respectively.

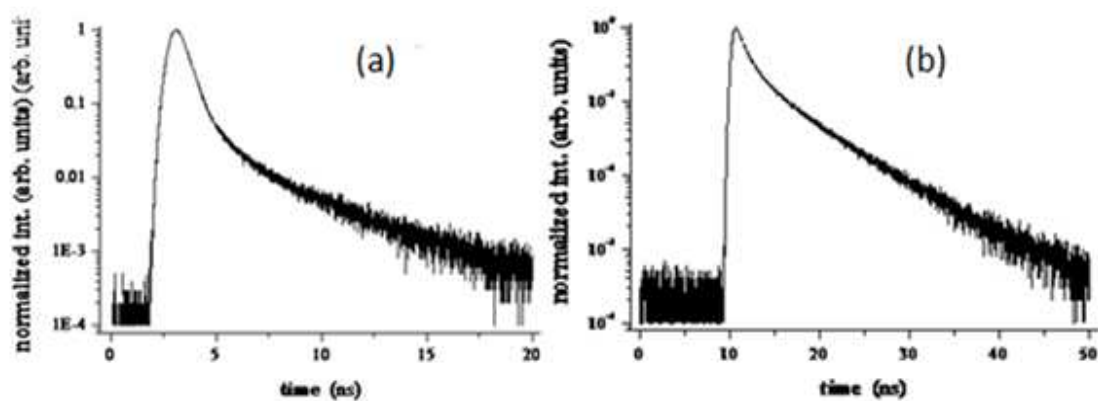


Fig. 14 Absorption (a) and emission (b) spectra of dye **Cou-Rh-1** (spirocyclic form) after the irradiation of UV light (254 nm) at different time intervals in toluene solvent (λ_{ex} : 375 nm).

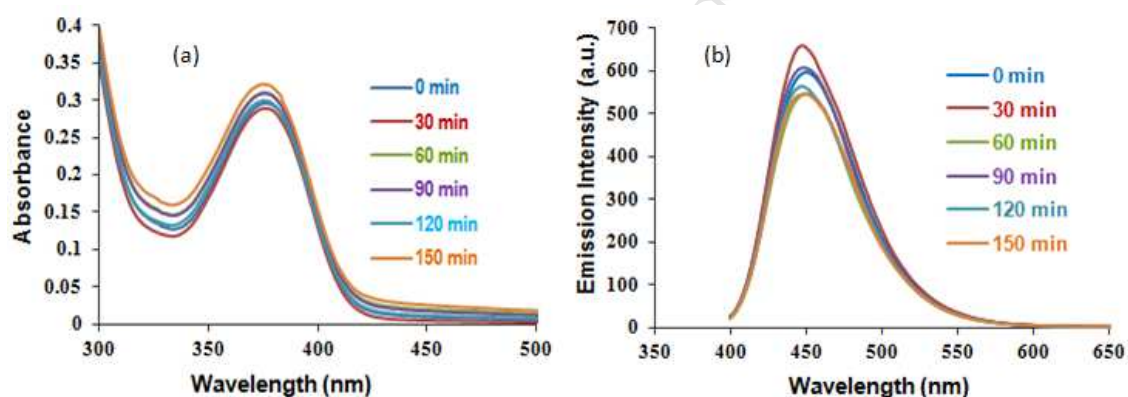
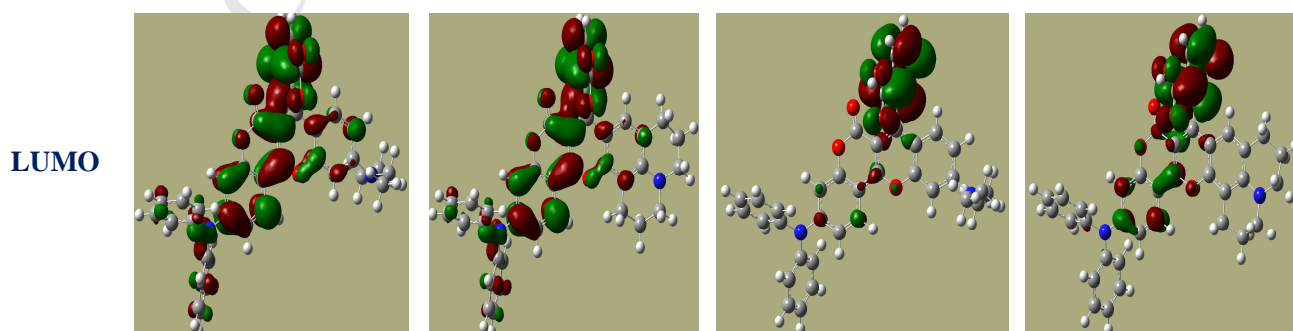


Fig. 15 HOMO-LUMO FMO diagrams of **Cou-Rh-1** and **Cou-Rh-2** dyes in their spirocyclic and open form in toluene and chloroform solvent respectively at ground state.



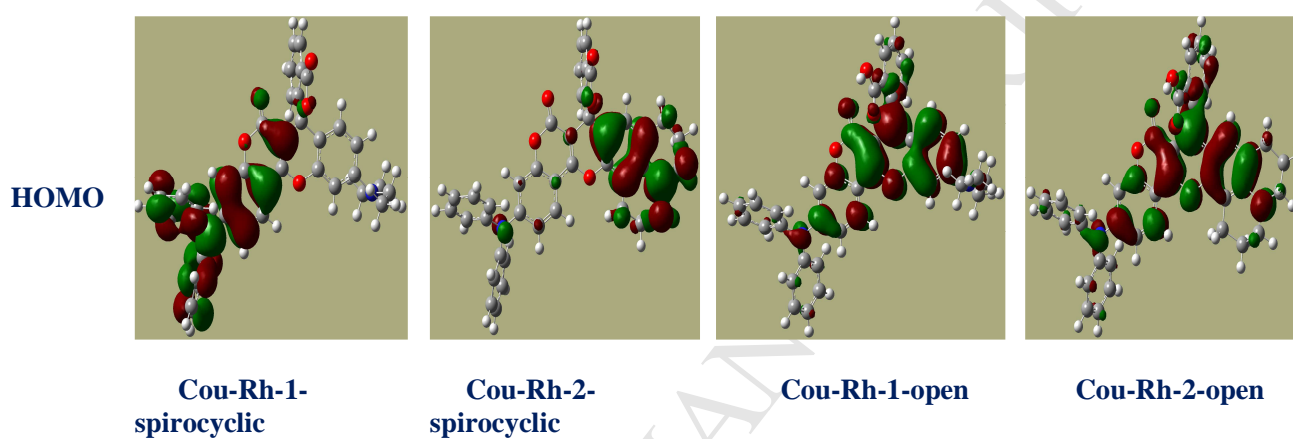
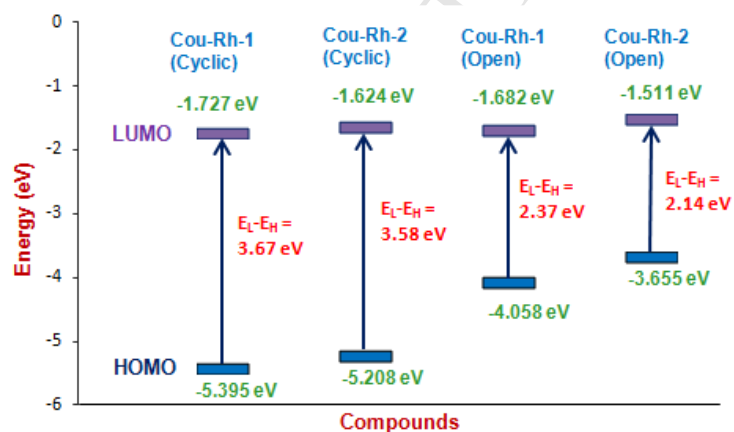


Fig. 16 HOMO-LUMO energy diagrams of **Cou-Rh-1** and **Cou-Rh-2** dyes in their spirocyclic and open form chloroform solvent.



Highlights

- Synthesis of triphenylamine based novel coumarin-rhodamine hybrid dyes.
- In their open form they show absorption and emission peaks in the deep red region.
- Larger Stokes shift than reported rhodamine dyes RH-B and RH-101 are found.
- They exhibit viscosity sensitivity in visible as well as deep red region.
- Solvent polarity and viscosity works together for the observed emission enhancement.